NUCL SCI TECH (2019) 30:12
https://doi.org/10.1007/s41365-018-0537-3

Thermal–hydraulic analysis of space nuclear reactor TOPAZ-II with modified RELAP5

Cheng-Long Wang[1] · Tian-Cai Liu[2] · Si-Miao Tang[1] · Wen-Xi Tian[1] · Sui-Zheng Qiu[1] · Guang-Hui Su[1]

Received: 7 August 2018 / Revised: 19 October 2018 / Accepted: 22 October 2018 / Published online: 2 January 2019

Abstract With the advantages of high reliability, power density, and long life, nuclear power reactors have become a promising option for space power. In this study, the Reactor Excursion and Leak Analysis Program 5 (RELAP5), with the implementation of sodium–potassium eutectic alloy (NaK-78) properties and heat transfer correlations, is adopted to analyze the thermal–hydraulic characteristics of the space nuclear reactor TOPAZ-II. A RELAP5 model including thermionic fuel elements (TFEs), reactor core, radiator, coolant loop, and volume accumulator is established. The temperature reactivity feedback effects of the fuel, TFE emitter, TFE collector, moderator, and reactivity insertion effects of the control drums and safety drums are considered. To benchmark the integrated TOPAZ-II system model, an electrical ground test of the fully integrated TOPAZ-II system, the V-71 unit, is simulated and analyzed. The calculated coolant temperature and system pressure are in acceptable agreement with the experimental data for the maximum relative errors of 8 and 10%, respectively. The detailed thermal–hydraulic characteristics of TOPAZ-II are then simulated and analyzed at the steady state. The calculation results agree well with the design values. The current work provides a solid foundation for space reactor design and transient analysis in the future.

Keywords Space nuclear reactor TOPAZ-II · Thermal–hydraulic analysis · RELAP5 modification

This work was supported by the China National Postdoctoral Program for Innovative Talents (No. BX201600124), China Postdoctoral Science Foundation (No. 2016M600796), and the National Natural Science Foundation of China (No. 11605131).

✉ Sui-Zheng Qiu
szqiu@mail.xjtu.edu.cn

[1] Department of Nuclear Science and Technology, Xi'an Jiaotong University, Xi'an 710049, China

[2] China Institute of Atomic Energy, Beijing 102413, China

1 Introduction

With the strong demand for space exploration, the requirement for nuclear power technology featuring high reliability, high power density, long service life, small volume, and lightweight in civil and military space missions is increasing. The former Soviet Union and USA have designed several types of space nuclear reactor systems including a thermoelectric conversion reactor system, thermionic conversion reactor system, Brayton cycle reactor system, and Stirling cycle reactor system [1–4]. The TOPAZ-II reactor system is the most advanced and experienced space nuclear power reactor based on thermionic conversion [5].

In the 1960s, extensive experimental research based on direct energy conversion technology was conducted by the former Soviet Union. The test program, including mechanical, thermal management, ground nuclear, and electrical heated thermal vacuum tests, was conducted to confirm the TOPAZ-II system's operational performance [6]. In the 1990s, a joint thermionic (TI) program between the Air Force and Department of Energy in the USA was established and tests of the TOPAZ-II system with electrical heated thermionic fuel elements (TFEs) were conducted at the Thermionic System Evaluation Test (TSET) facility [7]. The TOPAZ-II TFEs have undergone extensive testing with electrical heating to optimize the operational parameters [8].

In addition to experimental tests, numerical simulations have also been performed. The Thermionic Integrated Transient Analysis Model (TITAM) code was developed to investigate the steady and transient performance of a single-cell TFE with either fission or electrical heating [9]. The start-up process of TOPAZ-II and a non-credible start-up accident with TOPAZ-II prior to launch were simulated with the TITAM [10, 11]. The TOPAZ-II system responses under accident conditions were modeled by the Russian dynamics analytical simulator called ENSY. The accident conditions included switch failure during start-up, neutron regulator switch failure during start-up, and a loss of coolant accident (LOCA) [12]. The Code for Extended Nonlinear Transient Analysis of Extraterrestrial Reactors (CENTAR) was developed to quantify the operator's response time of the TSET following an interruption in vacuum chamber cooling [13]. The Transient Analysis code of Space Thermionic Nuclear reactor (TASTIN) was developed by Xi'an Jiaotong University to analyze the transient thermal–hydraulic characteristics of TOPAZ-II [14, 15].

RELAP5, as the best estimate transient simulation tool for reactors cooled by light water or heavy water, does not include the capability to perform the thermal–hydraulic analysis of the sodium–potassium eutectic alloy-cooled (NaK-78) space nuclear reactor owing to the lack of the related physical properties and heat transfer correlations of NaK-78. In this study, the thermodynamic and transport properties of NaK-78 and heat transfer correlations for liquid metals were implemented in the RELAP5 code. The RELAP5 model for TOPAZ-II including TFEs, reactor core, coolant loop, radiator, and volume accumulator was established. The TOPAZ-II ground test V-71 unit was simulated with the modified RELAP5 to verify and validate the developed model. Based on verification and validation, the steady state with nominal power and start-up procedures of TOPAZ-II were simulated and analyzed. This work aims to provide a valid method to conduct thermal–hydraulic analysis of space nuclear reactors.

2 TOPAZ-II description

The TOPAZ-II is a thermionic space reactor system that can generate 4.5–5.5 kW of electricity utilizing the in-core thermionic conversion units. The major subsystems of the TOPAZ-II are the (1) NaK-78-cooled reactor with epithermal neutron energy spectrum, (2) lithium hydride radiation shield, (3) electromagnetic (EM) pump for circulating the coolant, (4) radiator for waste heat rejection into space, (5) cesium reservoir assembly for supplying cesium vapor for the operation of the TFEs, and (6) instrumentation and control (I&C) system for regulating the reactor power. Figure 1 displays the TOPAZ-II schematic diagram.

The nuclear reactor incorporates 37 single-cell TFEs. Thirty-four of the TFEs are connected in series to provide electricity. The other three are connected in parallel to provide power for the electromagnetic (EM) pump. The reactor power can be controlled by rotating the three safety drums and nine control drums. A radial cross section of the TOPAZ-II reactor core is depicted in Fig. 2. The main design parameters of TOPAZ-II are summarized in Table 1. Additional TOPAZ-II system information can be found in Ref. [16].

3 RELAP5 modification and modeling

3.1 Thermo-physical properties of NaK-78

RELAP5 is coded in a modularized program using top-down structuring. The code top-level structure consists of the data input (INPUT), transient calculation (TRNCTL), and result stripping (STRIP) blocks. To simulate the NaK-78 alloy-cooled space reactors, subroutines in the INPUT and TRNCTL blocks must be modified. The thermo-physical properties of the NaK-78 alloy (78% K and 22% Na) are implemented into the RELAP5 code. The required

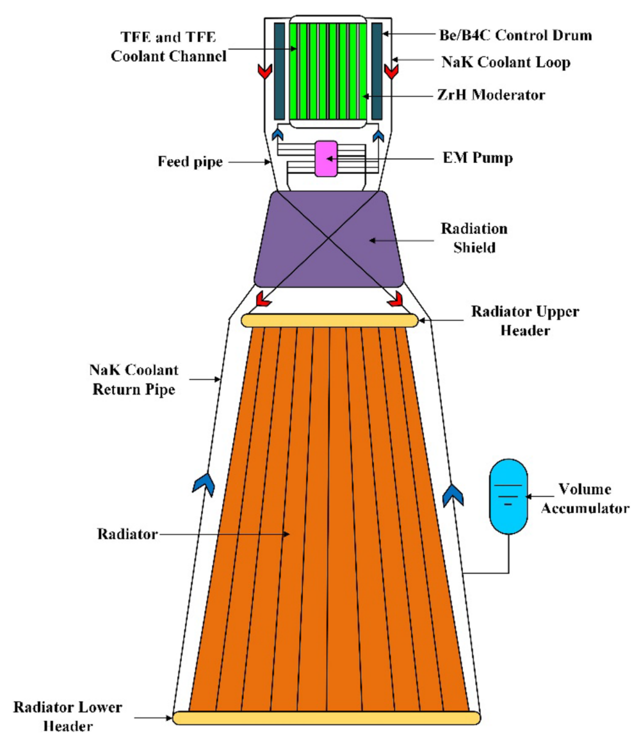

Fig. 1 (Color online) TOPAZ-II schematic diagram

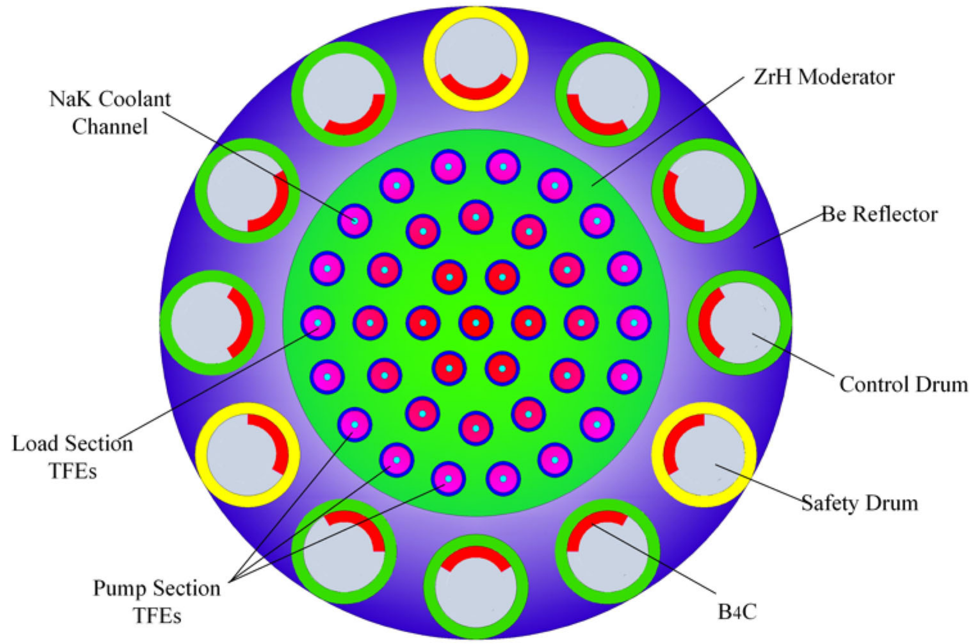

Fig. 2 (Color online) Radial cross section of TOPAZ-II reactor core

Table 1 Main design parameters of TOPAZ-II

Parameter	Value
Lifetime (year)	3
Thermal power at BOL/MAX (kWth)	115/135
TFEs electrical power (kWe)	4.5–5.5
Conversion efficiency at BOL	5.2%
Voltage (V)	27 ± 0.8
Reactor neutron spectrum	Epithermal
Reactor fuel	UO_2
Fuel enrichment	96% U-235
Fuel loading (kg)	27
Reactor core diameter (mm)	260
Reactor core height (mm)	375
Coolant type	NaK-78 (78% K, 22% Na)
Coolant temperature at core inlet (K)	743
Coolant temperature at core outlet (K)	843
Coolant mass flow rate (kg/s)	1.3
System pressure (MPa)	0.1
Radiator mass (kg)	46
Number of radiator elements	78
Radiator fin material	Copper with black enamel coating
Radiator surface (m^2)	7.2
Radiator emissivity	0.86
Reactor control	9 control drums and 3 safety drums
Moderator	$ZrH_{1.85}$
Primary system material	Stainless steel
TFE emitter material	Monocrystal Mo with 3% Nb
TFE collector material	Polycrystal Mo
Shield material	LiH for neutron and stainless steel for gamma
Number of TFE elements in core	37

properties are the isothermal compressibility, specific volume, thermal expansion coefficient, specific enthalpy, specific heat capacity and transport properties of thermal conductivity, surface tension, and dynamic viscosity.

Based on Raoult's law, the vaporization curve of NaK-78 can be expressed as [17]:

$$\lg(P/1.3) = 9 - 4367/T, \tag{1}$$

where P is the pressure (Pa) and T is the temperature (K).

3.1.1 Liquid thermo-physical properties

The density of the liquid NaK-78 alloy changes with temperature. It was reported by Qian [18], and the linear fitted formulation can be expressed as the following form with 1% maximum error:

$$\rho_l = 946.65 - 0.245 \times T, \tag{2}$$

where ρ_l is the liquid density (kg/m^3).The specific volume υ_l is

$$\upsilon_l = 1/\rho_l. \tag{3}$$

The adiabatic compressibility of liquid NaK-78 is related to sound speed and can be expressed as in Eq. (4). The isothermal compressibility of NaK-78 is related to the adiabatic compressibility and can be defined as in Eq. (5).

$$k_s = 1/(\rho c^2), \tag{4}$$

$$k_t = k_s + (T\alpha^2)/(\rho c_p), \tag{5}$$

where k_s is the adiabatic compressibility (Pa^{-1}), k_t is the isothermal compressibility (Pa^{-1}), c is the sound speed (m/s), c_p is the specific heat capacity [J/(kg K)], α is the thermal expansion coefficient (K^{-1}), and ρ is the density (kg/m^3).

The sound speed of liquid NaK-78 can be expressed as

$$c = 1906.2 - 0.53\,T. \tag{6}$$

The coefficient of thermal expansion can be obtained from Eq. (7).

$$V = V_0[1 + \alpha(T - 273)], \tag{7}$$

where V is the volume of liquid NaK-78 and V_0 is the volume of liquid NaK-78 at 273 K. The thermal expansion coefficient α is assumed to be a constant of 2.77×10^{-4} K^{-1}.

The specific heat capacity of NaK-78 can be obtained from the following equation [19]:

$$c_p = 1097.04 - 0.556T + 3.431 \times 10^{-4}T^2. \tag{8}$$

The specific enthalpy of liquid NaK-78 can be expressed as the following form:

$$\begin{aligned} h_l = {} & 938.6 \times (T - 273) - 1.0962 \times 10^{-6}(T - 273)^2 \\ & + 7.0555 \times 10^{-5}(T - 273)^3 + 0.05636 \times (T - 273) \\ & \times e^{-0.004055\times(T-273)}, \end{aligned} \tag{9}$$

where h_l is the specific enthalpy (J/kg). Equation (9) is fitted with the experimental data with 0.3% maximum error. The specific internal energy u_l can be obtained by

$$u_l = h_l - P \cdot \upsilon_l. \tag{10}$$

The differential equation of specific entropy can be expressed as [20]

$$\mathrm{d}s = \frac{c_p}{T}\mathrm{d}T - \left(\frac{\partial \upsilon}{\partial T}\right)_P \mathrm{d}P. \tag{11}$$

Substituting specific volume and specific heat capacity into Eq. (11) and integrating the equation, the liquid specific entropy can be expressed as

$$\begin{aligned} s_l = {} & c_p \ln(T/T_0) + s_{l0} - 0.245(P - P_0) \cdot (946.65 \\ & - 0.245T)^{-2}, \end{aligned} \tag{12}$$

where s_{l0} is the reference liquid specific entropy at T_0 and P_0, c_p is the specific heat capacity [J/(kg K)], and s_l is the specific entropy [J/(kg K)].

3.1.2 Vapor thermo-physical properties

In TOPAZ-II, the coolant temperature ranges from 300 K to 850 K during the start-up and normal operation; the phenomena of coolant boiling is expected to be avoided during the accident scenarios. Therefore, the vapor NaK-78 alloy is not important and is simplified as the ideal gas.

The vapor density of NaK-78 can be calculated as follows:

$$\rho_g = \frac{P}{R \cdot T}, \tag{13}$$

where R represents the gas constant and is 229.26 J/(kg K).

Similarly, the specific enthalpy for vapor NaK-78 can be represented as

$$h_g = c_{pg}(T - T_0) + h_{g0}, \tag{14}$$

where h_{g0} is the reference vapor specific enthalpy at T_0 and P_0.

The vapor specific internal energy can be expressed as

$$u_g = h_g - P \cdot \upsilon_g. \tag{15}$$

The specific entropy of vapor NaK-78 can be calculated as

$$s_g = c_{pg} \ln\left(\frac{T}{T_0}\right) - R \ln\left(\frac{P}{P_0}\right) + s_{g0}, \tag{16}$$

where s_{g0} represents the vapor specific entropy at the triple point and s_g is the specific entropy [J/(kg K)].

3.2 Transport properties

Transport properties including the thermal conductivity λ [W/(m K)], surface tension σ [N/m], and dynamic viscosity μ (Pa s) are required in the RELAP5 code modification.

The thermal conductivity of liquid NaK-78 is implemented as [19]

$$\lambda = 14.11 + 0.0327T - 2.2 \times 10^{-5}T^2. \tag{17}$$

Equation (17) is mainly in terms of the experimental data, with 0.8% maximum error.

The surface tension of the liquid NaK-78 changed with temperature can be obtained in terms of the surface tension of sodium and potassium. The linear fitted formulation can be expressed as

$$\sigma = 1.357 - 7.192 \times 10^{-5}(T - 273). \tag{18}$$

The dynamic viscosity of NaK-78 can be expressed as

$$\begin{cases} \mu = 0.116\rho^{1/3}\exp(668\rho/T),\ T \le 773\,K \\ \mu = 8.2 \times 10^{-2}\rho^{1/3}\exp(979\rho/T),\ T > 773\,K \end{cases}. \tag{19}$$

3.3 Heat transfer correlations for liquid metal

In the modified RELAP5, the heat transfer correlation [21] for the liquid metal convection heat transfer in tube is

$$Nu = 6.0 + 0.025\left[0.014Re^{0.45}Pr^{0.2}\left(1 - e^{-\frac{71.8}{Re^{0.45}Pr^{0.2}}}\right)Pe\right]^{0.8}, \tag{20}$$

where Nu represents the Nusselt number, Re is the Reynolds number, Pr represents the Prandtl number, and Pe represents the Peclet number. Equation (20) is appropriate to fully develop the flow, and the Nusselt number for the laminar flow regime in tube is

$$Nu = 4.36 \quad \text{for} \quad Re < 3000. \tag{21}$$

The convection heat transfer correlation [22] for annular pipes with liquid metals is

$$\begin{cases} Nu = 5.25 + 0.0188Pe^{0.8}(D_2/D_1)^{0.3}, D_2/D_1 > 1.4 \\ Nu = 5.8 + 0.02Pe^{0.8}, D_2/D_1 \to 1 \end{cases}, \tag{22}$$

where D_1 is the inner diameter and D_2 is the external diameter.

The convection heat transfer correlation [23] for rod bundles with liquid metals is

$$Nu = 4.0 + 0.16(P/D)^{5.0} + 0.33(P/D)^{3.8}(Pe/100)^{0.86} \quad \text{for} \quad 1.1 < P/D < 1.4 \quad 10 < Pe < 5000, \tag{23}$$

where P/D is the rod or tube pitch-to-diameter ratio.

3.4 RELAP5 modeling

The RELAP5 model for the TOPAZ-II system was developed, and the nodalization of the TOPAZ-II system is presented in Fig. 3. The established model contains virtually all the main structures including in-core TFEs, reactor core, pump, radiator, primary loop, and volume accumulator. Owing to the TFE layout symmetry, the TFEs in the same circumference were simplified as one coolant channel in the RELAP5 model. Thirty-seven TFEs were divided into four coolant channels including 1, 6, 12, and 18 TFEs, respectively, as indicated in Fig. 4. They were modeled as components 210, 220, 230, and 240. Components 210, 220, 230, and 240 are annulus-type hydraulic components with 24.5 mm inner diameter, 25.9 mm outer diameter, and 375 mm height. In the RELAP5 model, coolant Channel 1 was defined as a hot channel; the other three coolant channels were simplified as average channels. Both sides of a coolant channel were coupled with heat structures. The complex TFE ring structures of fuel, fission gas gap, emitter, cesium gap, collector, helium gap, stainless steel inner wall, stainless steel outer wall, CO_2 gap and ZrH moderator were modeled in the heat structures with an

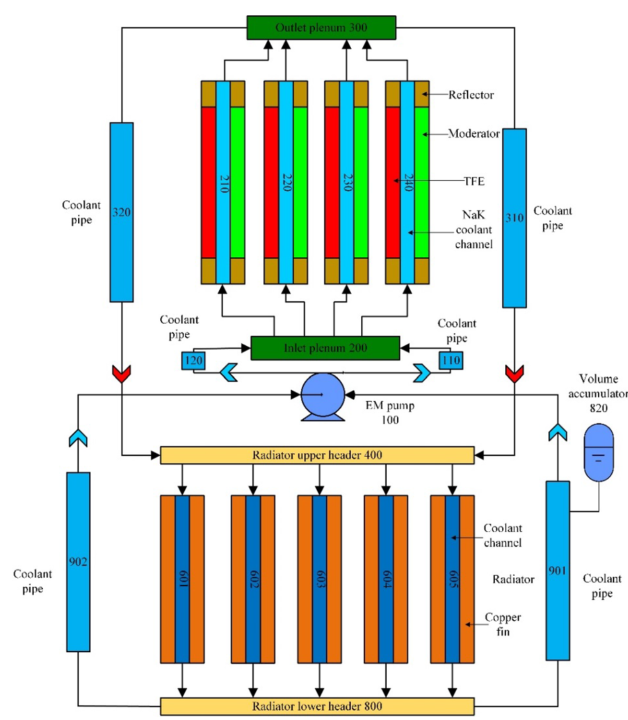

Fig. 3 (Color online) Nodalization of TOPAZ-II

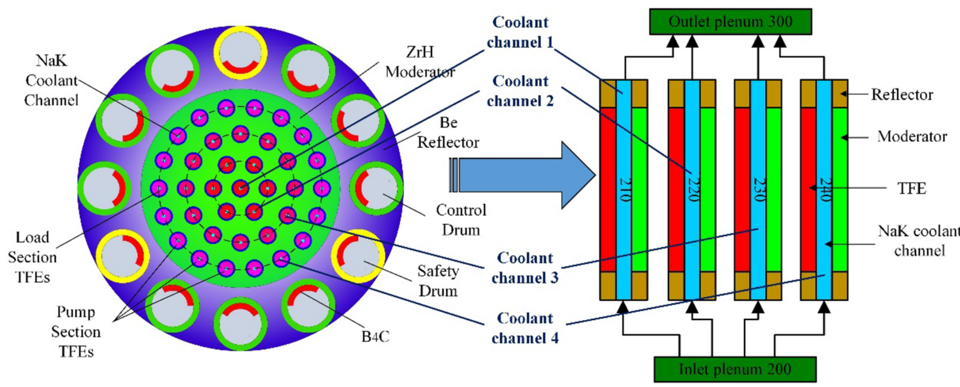

Fig. 4 (Color online) Schematic of core simplification process

outer diameter of 17 mm, 17.3 mm, 19.6 mm, 20.6 mm, 23.4 mm, 23.8 mm, 24.5 mm, 26.6 mm, 27.5 mm, and 37.1 mm, respectively. A schematic of the TFE cross section is presented in Fig. 5.

The radiator is an uncommon component compared to a convection nuclear system. The radiator consists of an upper header, lower header, and 78 radiator coolant channels (as indicated in Fig. 1). The radiator fin material is copper with black enamel coating, and the effective radiator surface is 7.2 m^2. The upper header (Component 400) and lower header (Component 800) of the radiator are circular ring structures. The radiator is a circular cone-truncated structure. Owing to the symmetry of the headers and radiator, the 78 coolant channels in the radiator were simplified into 20 channels divided into four groups based on the coolant flow direction in the upper header. Each group corresponds to a coolant flow direction and contains five coolant channels in parallel with equivalent flow area. The coolant channel is 22.1 mm in diameter and 1830 mm in height. The radiator model displayed in Fig. 3 is only one group of radiator parallel channels. The other three groups of radiator parallel channels exist in the RELAP5 model; however, they are not displayed in Fig. 3. The outsides of the radiator coolant channels have rectangular-type heat structures to model the copper fins. The surface radiation emissivity of the copper fins is 0.86. The top view of radiator and the radiator simplification process are displayed in Fig. 6. The detailed hydraulic components illustrated are listed in Table 2.

4 Results and discussion

4.1 Verification and validation

To benchmark the fully integrated TOPAZ-II system model, the model predictions were compared with the steady-state measurements for an electrically heated, fully integrated TOPAZ-II system, the V-71 unit. The V-71 unit is the first electrically heated ground test of a complete thermionic space nuclear power system [24]. For the V-71 unit, the fuel pellets were replaced by electrically heated tungsten; the thermal heat flux to the emitter was assumed uniform along the active emitter.

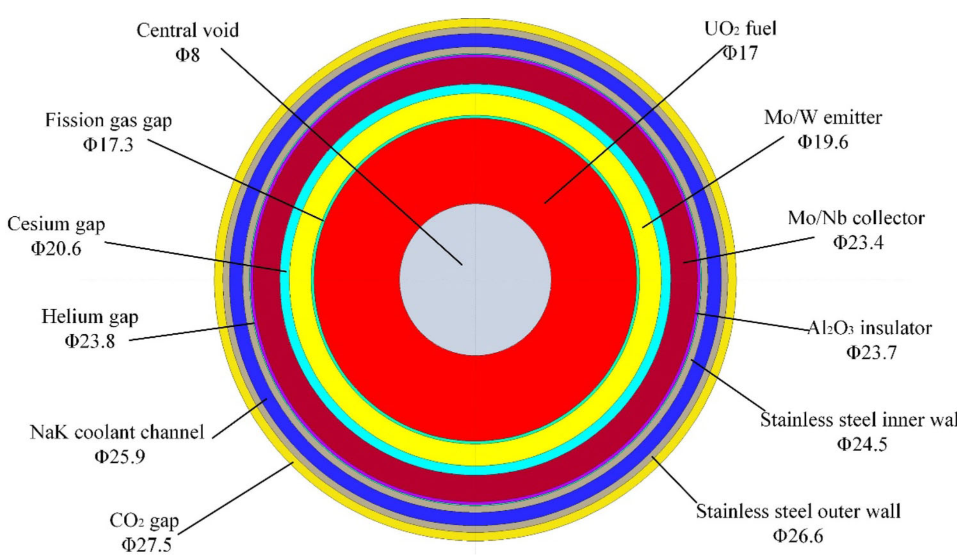

Fig. 5 (Color online) Schematic of TFE cross section

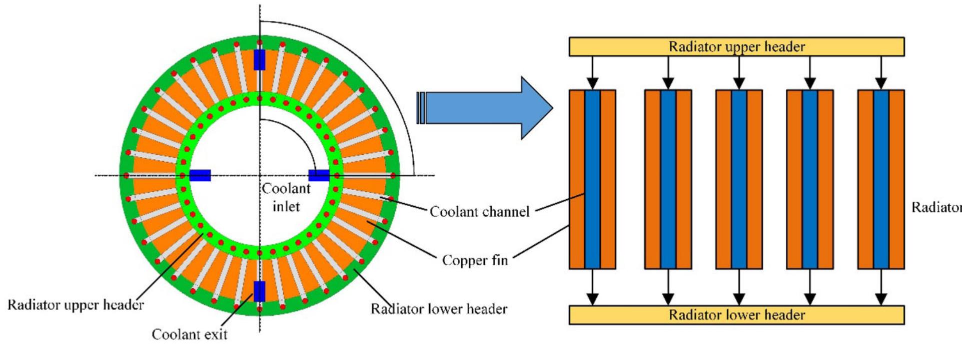

Fig. 6 (Color online) Top view of radiator and schematic of radiator simplification process

Table 2 TOPAZ-II model components description

Component	Component type and geometrical information
100	Time-dependent junction: EM pump
110, 120	Pipe: coolant pipe from EM pump to inlet plenum (1.73×10^{-3} m^3 in flow area, 2.93 m in height)
200	Branch: core inlet plenum (6.9×10^{-3} m^3 in flow area, 0.014 m in height)
210	Pipe: hot channel (5.54×10^{-5} m^3 in flow area, 0.375 m in height)
220, 230, 240	Pipe: average channel (5.54×10^{-5} m^3 in flow area, 0.375 m in height)
300	Branch: core outlet plenum (6.9×10^{-3} m^3 in flow area, 0.014 m in height)
310, 320	Pipe: coolant pipe from core outlet plenum to radiator upper header (8.67×10^{-4} m^3 in flow area, 2.93 m in height)
400	Branch: radiator upper header (3.62×10^{-3} m^3 in flow area, 0.73 m in length)
601–605	Pipe: radiator coolant channel (3.85×10^{-4} m^3 in flow area, 1.83 m in height)
800	Branch: radiator lower header (8.67×10^{-4} m^3 in flow area, 3.93 m in length)
820	Time-dependent volume: volume accumulator
901, 902	Pipe: coolant pipe from radiator lower header to EM pump (1.73×10^{-3} m^3 in flow area, 3.85 m in height)

The comparisons of the calculated and measured coolant temperatures at the core inlet and core outlet are displayed in Fig. 7. The calculated values are in acceptable agreement with the experimental data. The maximum relative error is 8% as indicated in Fig. 8. The error between the calculated results and the experimental data can be caused by the error of the coolant mass flow rate. The comparison of the calculated and measured system pressure is displayed in Fig. 9. The maximum relative error is 10% as

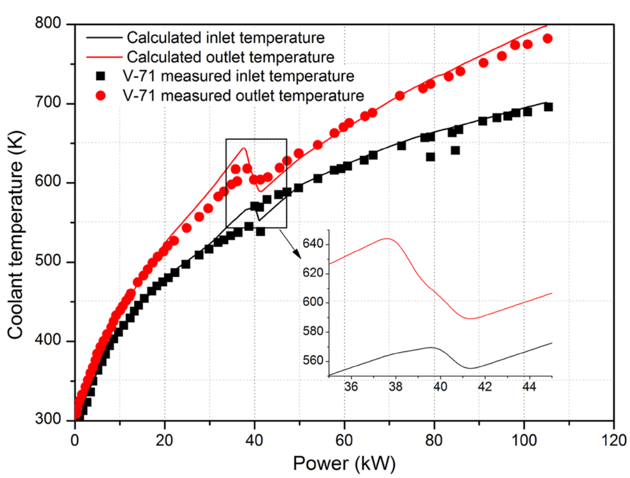

Fig. 7 (Color online) Comparison of calculated and measured coolant temperature of V-71 unit

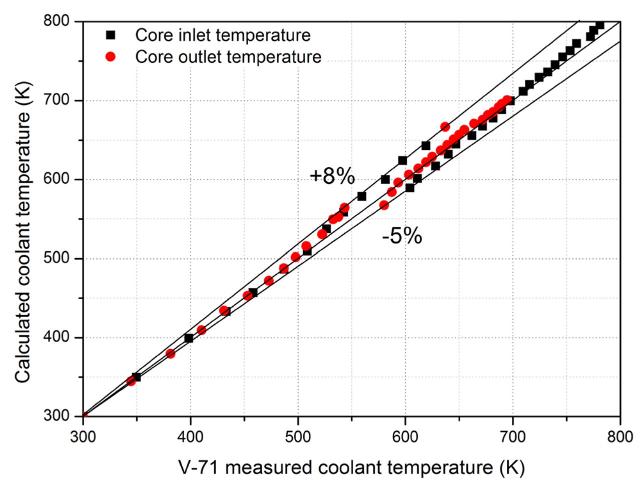

Fig. 8 (Color online) Relative error of calculated and measured coolant temperature of V-71 unit

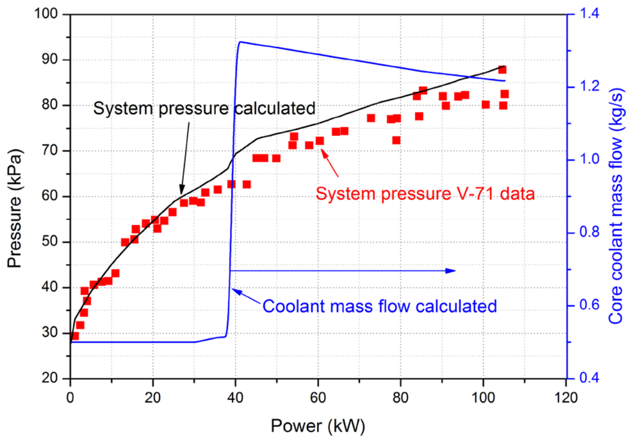

Fig. 9 (Color online) Comparison of calculated and measured system pressure and coolant mass flow of V-71 unit

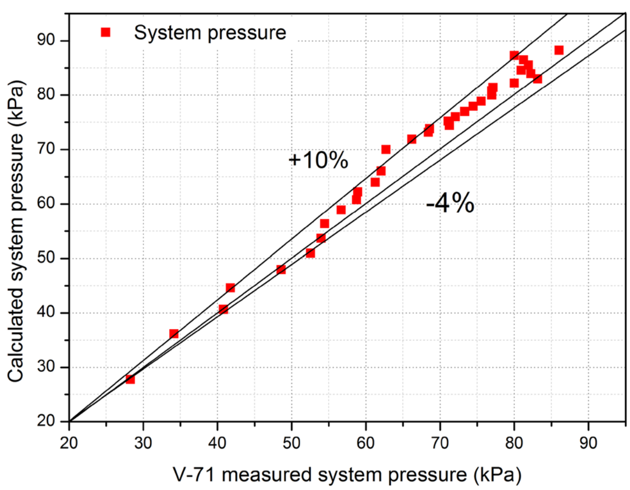

Fig. 10 (Color online) Relative error of calculated and measure system pressure of V-71 unit

indicated in Fig. 10. The system pressure mainly influences the subcooling degree of the coolant, which is approximately 300 K in normal operation; hence, the maximum relative error of 10% in the local region is acceptable.

4.2 Steady-state analysis

The steady-state analysis of TOPAZ-II was performed with the modified RELAP5. The comparisons between the steady-state results and design values are presented in Table 3; the calculated results agree well with the design values.

The radial temperature distribution of the TFE at different positions in the average coolant channel is displayed in Fig. 11. Five typical positions are indicated in Fig. 11. The fuel maximum temperature of 1941 K appears in the fuel center of Position 2. Because the thermal conductivity of the cesium vapor is low and electric power is generated between emitters and collectors, a clear temperature reduction appears in the cesium vapor gap. Owing to the high thermal conductivity coefficient and large heat capacity, the radial temperature distribution in the moderator is uniform. The radial temperature distribution in the reflector is smooth, and the temperature distribution is virtually the same as the coolant temperature.

Figures 12 and 13 display the axial temperature distribution of each TFE component in the hot channel. The axial temperature distribution of the fuel pellets depends on the axial power curve and radial heat conduction. A maximum fuel pellet temperature of 2039 K appears in the middle of the fuel, which is considerably less than the melting temperature of approximately 3100 K. The axial temperature distribution of the fission gas and emitter is mainly determined by the radial heat conduction from the fuel pellets. The temperature variation trend is consistent with the fuel temperature distribution. Owing to the low thermal conductivity of cesium vapor, the temperature distribution of the components outside the cesium vapor is less influenced by the fuel temperature distribution and more influenced by the coolant axial temperature distribution.

Figure 14 illustrates the coolant temperature distributions along the flow direction in four coolant channels and two radiator channels. The core coolant Channel 1 is the hot channel; the other three channels are average channels. The outlet coolant temperature in the hot channel is 10 K higher than that in the average channel outlet. The maximum coolant temperature is 854 K, which is considerably less than its saturation temperature of approximately

Table 3 Comparison of design value and calculated value of TOPAZ-II

Parameter	Design value	Calculated value
Reactor thermal power (kW) (fixed parameter)	115	115
Coolant temperature at core inlet (K)	743	744
Coolant temperature at core outlet (K)	843	844
Coolant mass flow rate (kg/s) (fixed parameter)	1.32	1.32

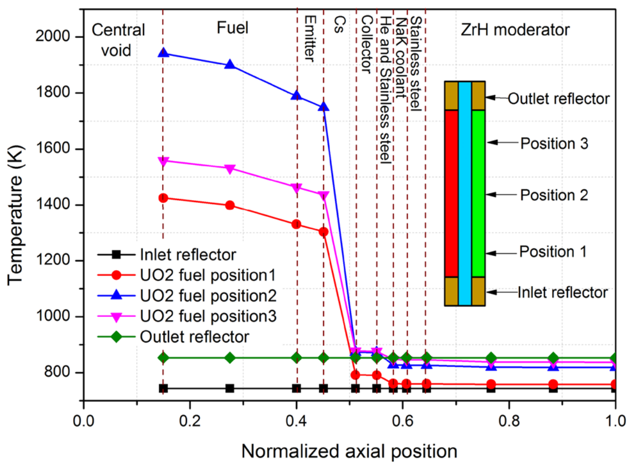

Fig. 11 (Color online) Radial temperature distributions at TFE different positions

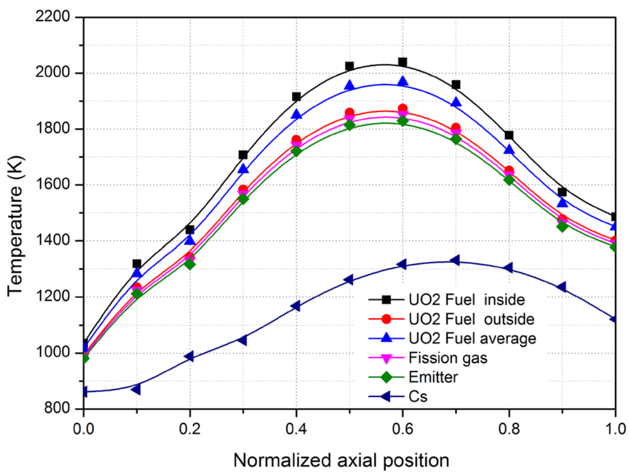

Fig. 12 (Color online) Axial temperature distribution of each component inside collector in hot channel TFE

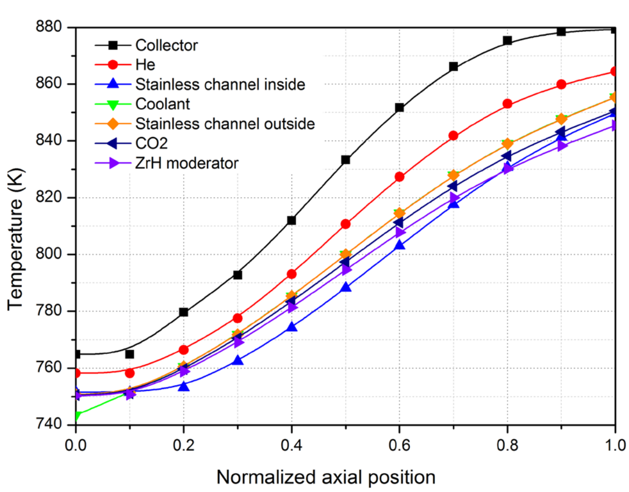

Fig. 13 (Color online) Axial temperature distribution of each component outside collector in hot channel TFE

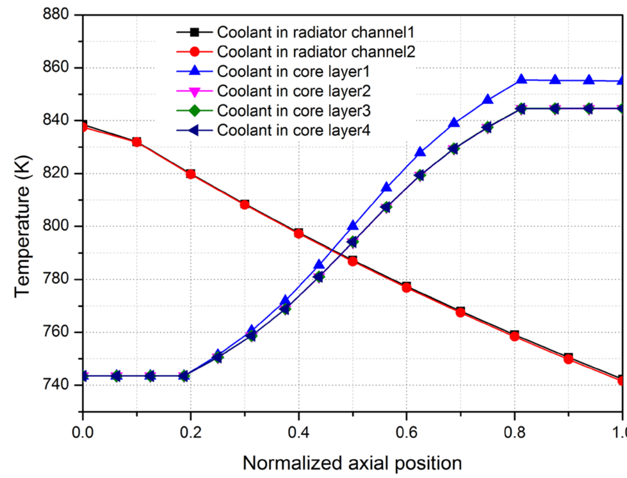

Fig. 14 (Color online) Coolant temperature axial distributions in core coolant channels and radiator channels

1100 K. The coolant temperature increase in the core is approximately 101 K, and the coolant temperature decrease in the radiator is approximately 96 K. This is because approximately 5% of the heat is radiated into space from the primary hot leg and cold leg. The coolant temperature has no change in core inlet reflector and core outlet reflector.

Figure 15 presents the local coolant temperature, coolant saturation temperature, and coolant subcooling degree of the primary system. The coolant is heated in the core, the core average channel outlet temperature attains a maximum of 844 K, and the coolant subcooling degree reaches a minimum of 260 K. There is a small amount of heat loss by radiation from the coolant pipes; the coolant temperature decreases marginally along the coolant flow direction. As the coolant flows through the radiator, the coolant temperature decreases to 746 K. When the coolant flows through the pump, the increase in the system pressure

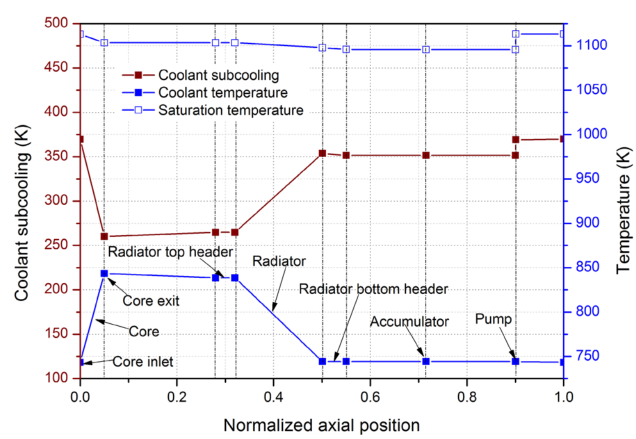

Fig. 15 (Color online) Local coolant temperature and coolant subcooling degree of TOPAZ-II

increases the coolant saturation temperature. The coolant temperature reaches a minimum value of 744 K after flowing through the pump. Therefore, the maximum value of coolant subcooling, in degrees, 370 K, occurs at the outlet of the EM pump. It can be concluded that the steady-state operation of TOPAZ-II is safe and reliable because of the higher design margin.

5 Conclusion

In this study, the thermo-physical properties and transport properties of NaK-78 and the relevant heat transfer correlations were implemented into the RELAP5 code. After modification, the modified RELAP5 was adopted to simulate and analyze the TOPAZ-II reactor system. A RELAP5 model including the core, TFEs, radiator, coolant loop, and volume accumulator was established. The ground test of the TOPAZ-II system, the V-71 unit, was adopted to benchmark the modified RELAP5 model. The steady-state condition of TOPAZ-II was simulated and analyzed. Based on the above analysis, the following conclusions can be obtained:

1. The V-71 unit was simulated using the modified RELAP5 with a comparison of the experimental data. The maximum relative error of the coolant temperatures was 8%, and the maximum relative error of the system pressure was 10%. Further, the maximum error only occurred in special positions around 40 kW. The acceptable agreement between the calculated results and experimental data preliminarily verifies and validates the modified RELAP5 model. This proves the capability of the modified RELAP5 to analyze the TOPAZ-II system.
2. The steady-state calculated results agree well with the reactor-designed values. The maximum coolant outlet temperature was 854 K, which has a large margin of approximately 250 K to the boiling point. The fuel maximum temperature was 2039 K, which is considerably less than the melting temperature of approximately 3100 K. This proves the good safety performance of the designed TOPAZ-II at the steady state. The transient safety characteristics should be assessed as a next step.

This work provides a solid foundation for a space nuclear reactor design and transient analysis in the future.

References

1. L.S. Mason, A comparison of Brayton and Stirling space nuclear power systems for power levels from 1 kilowatt to 10 megawatts. AIP Conf. Proc. **552**(1), 1017 (2001). https://doi.org/10.1063/1.1358045
2. G.L. Bennett, R.J. Hemler, A. Schock, Space nuclear power: an overview. J. Propul. Power **12**(5), 901 (1996). https://doi.org/10.2514/3.24121
3. D. Buden, Summary of space nuclear reactor power systems (1983–1992). Idaho National Engineering Laboratory Report (1993), Report ID: INEL/MISC-93085. https://inis.iaea.org/collection/NCLCollectionStore/_Public/25/070/25070118.pdf
4. A.J. Glassman, Summary of Brayton cycle analytical studies for space-power system applications. Sol. Energy. **7** (1964). https://ntrs.nasa.gov/archive/nasa/casi.ntrs.nasa.gov/19640020187.pdf
5. R.S Dabrowski, US-Russian Cooperation in science and technology: A case study of the TOPAZ space-based nuclear reactor international program. Connect. Q. J. **13**(1), 71 (2013). http://procon.bg/bg/system/files/13.1.05_dabrowski.pdf
6. S.S. Voss, E.A. Rodriguez, Russian TOPAZ II system test program (1970–1989). AIP Conf. Proc. **301**(1), 803 (1994). https://doi.org/10.1063/1.2950273
7. J.F. Fairchild, J.P. Koonmen, F.V. Thome, Thermionic system evaluated test (TSET) facility description. AIP Conf. Proc. **246**(1), 836 (1992). https://doi.org/10.1063/1.41884
8. V.P. Nicitin, B.G. Ogloblin, A.N. Luppov et al., Special features and results of the ''TOPAZ II'' nuclear power system tests with electric heating. AIP Conf. Proc. **246**(1), 41 (1992). https://doi.org/10.1063/1.41803
9. M.S. El-Genk, H. Xue, C. Murray et al., TITAM thermionic integrated transient analysis model: load-following of a single-cell TFE. AIP Conf. Proc. **246**(1), 1013 (1992). https://doi.org/10.1063/1.41776
10. M.S. El-Genk, D.V. Paramonov, A.C. Marshall, Startup simulation of the TOPAZ-II Reactor system for accident conditions. AIP Conf. Proc. **301**(1), 1059 (1994). https://doi.org/10.1063/1.2950104
11. M.S. El-Genk, H. Xue, D.V. Paramonov, Start-up simulation of a thermionic space nuclear reactor system. AIP Conf. Proc. **271**(2), 935 (1993). https://doi.org/10.1063/1.43119
12. S.S. Voss, The TOPAZ II space reactor response under accident conditions. Presented at the International Topical Meeting on the Safety of Advanced Reactors, Pittsburgh, PA, 18–20 Apr. 1994. https://www.osti.gov/biblio/10115301
13. V.H. Standley, D.B. Morris, M.J. Schuller, CENTAR modeling of the TOPAZ-II: loss of vacuum chamber cooling during full power ground test. AIP Conf. Proc. **246**(1), 1129 (1992). https://doi.org/10.1063/1.41770
14. W.W. Zhang, Z.Y. Ma, D.L. Zhang et al., Transient thermal–hydraulic analysis of a space thermionic reactor. Ann. Nucl. Energy **89**, 38 (2016). https://doi.org/10.1016/j.anucene.2015.10.035
15. W.W. Zhang, D.L. Zhang, W.X. Tian et al., Thermal-hydraulic analysis of the improved TOPAZ-II power system using a heat pipe radiator. Nucl. Eng. Des. **307**, 218 (2016). https://doi.org/10.1016/j.nucengdes.2016.07.020
16. S.S. Voss, TOPAZ-II system description, in *Proceedings of the Fourth International Conference on Engineering, Construction, and Operations in Space*, Albuquerque, NM. 717 (1994). https://inis.iaea.org/collection/NCLCollectionStore/_Public/25/040/25040534.pdf
17. C.B. Jackson, Liquid metals handbook. Sodium-NaK Supplement. Atomic Energy Commission, Washington, DC; Bureau of

Ships, Report ID: TID-5277 (1955). https://www.osti.gov/biblio/4376530
18. Z.Y. Qian, *Thermal Properties of Low Melting Point Metals* (Science Press, China, 1985). **In Chinese**
19. O.J. Foust, *Sodium-NaK engineering handbook* (Gordon & Breach Science Pub, New York, 1972)
20. M. Zemansky, R. Dittman, *Heat and Thermodynamics* (McGraww-Hill Inc Pub, New York, 1997)
21. S. Aoki, O.E. Dwyer, Current liquid-metal heat transfer research in Japan. Tokyo Inst. of Tech., Report ID: NSA-29-000316. 1973. https://www.osti.gov/biblio/4423836
22. O.E. Dwyer, P.S. Tu, Bilateral heat transfer to liquid metals flowing turbulently through annuli. Nucl. Sci. Eng. **21**(1), 90 (1965). https://doi.org/10.13182/NSE65-A21018
23. N.E. Todreas, M.S. Kazimi, *Nuclear systems: thermal hydraulic fundamentals* (CRC Press, Boca Raton, 2012), p. 306
24. D.V. Paramonov, M.S. El-Genk, Comparison of a TOPAZ-II Model with experimental data from the V-71 unit tests. AIP Conf. Proc. **301**(1), 829 (1994). https://doi.org/10.1063/1.2950277